SUPPLEMENTARY MATERIALS

Supplementary Materials included in this document:

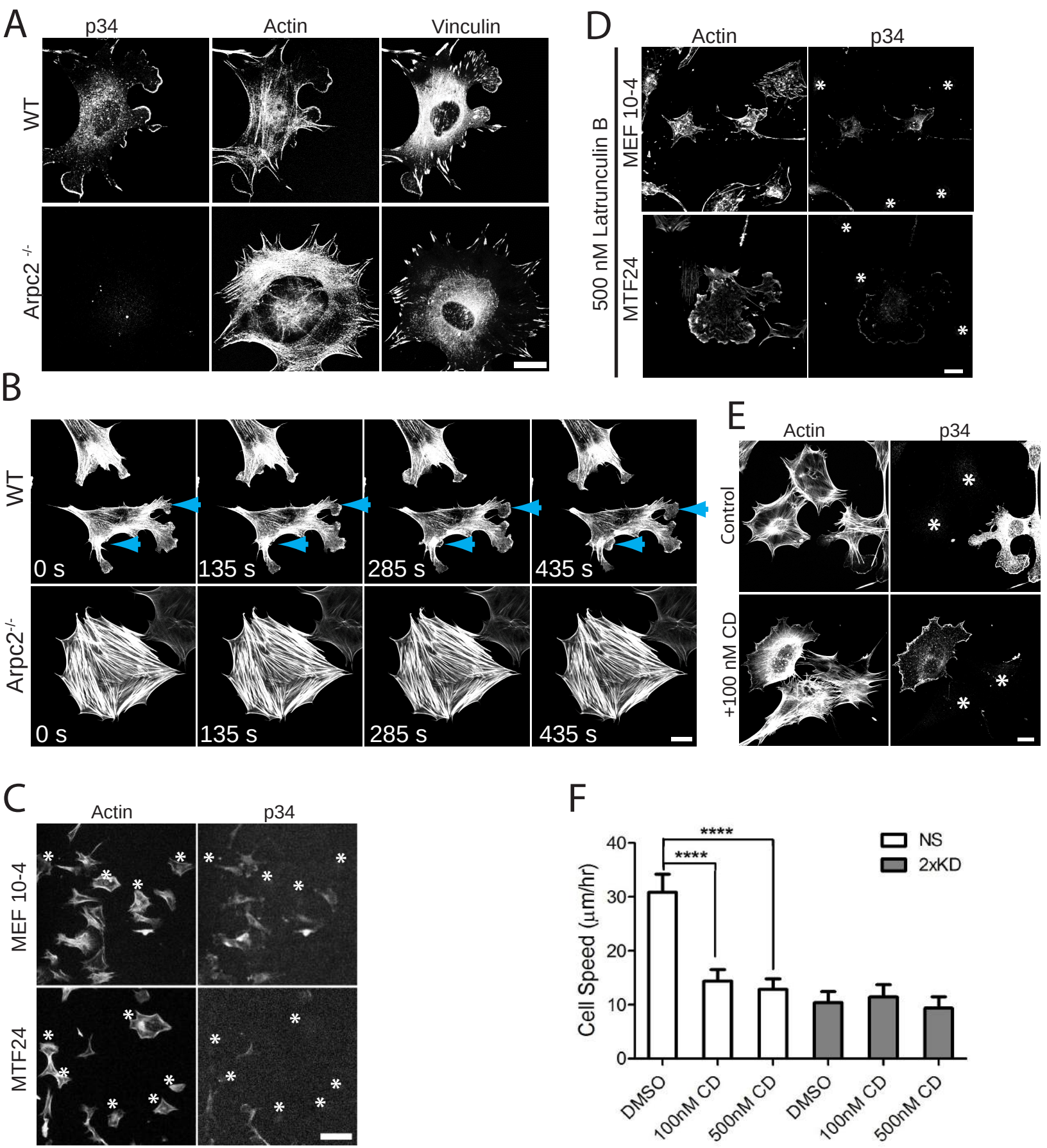

Rotty et al. Supplemental Figure 1

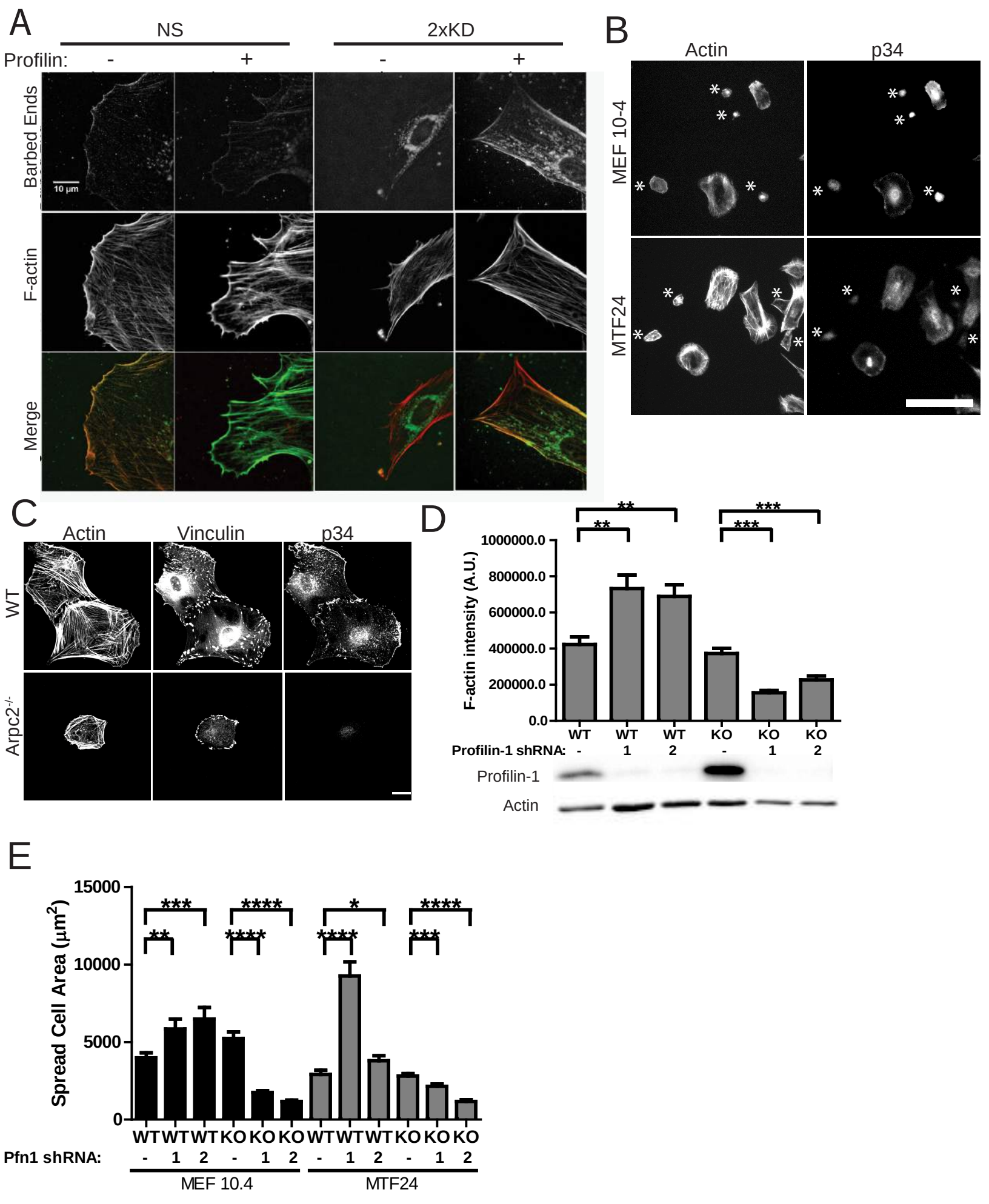

Rotty et al. Supplemental Figure 2

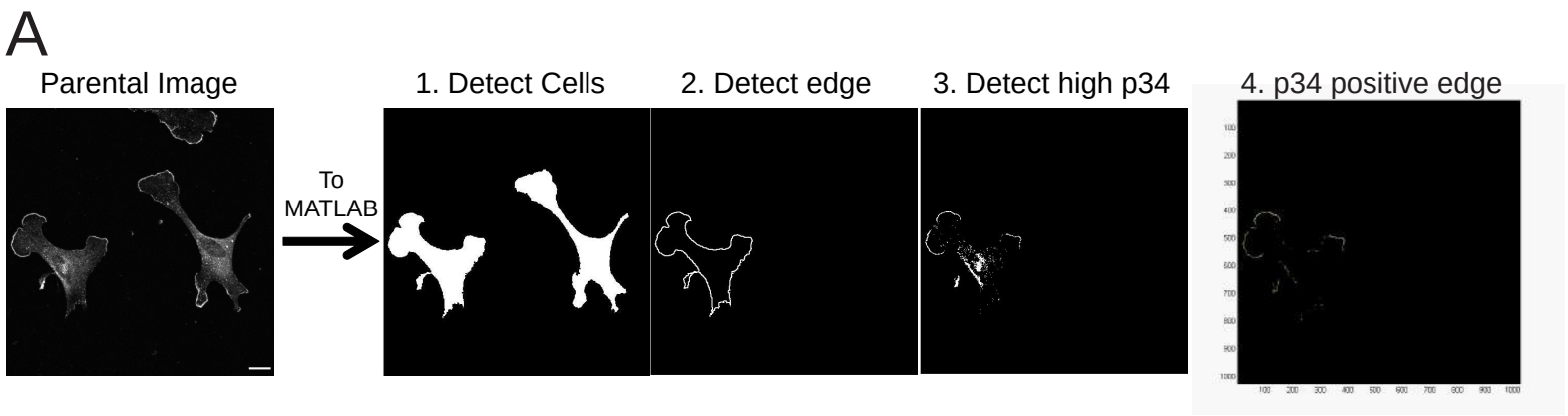

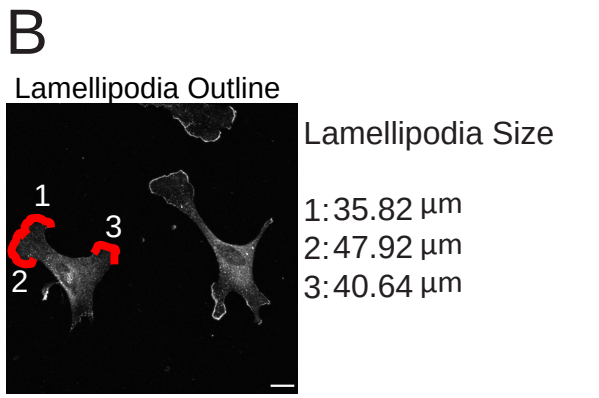

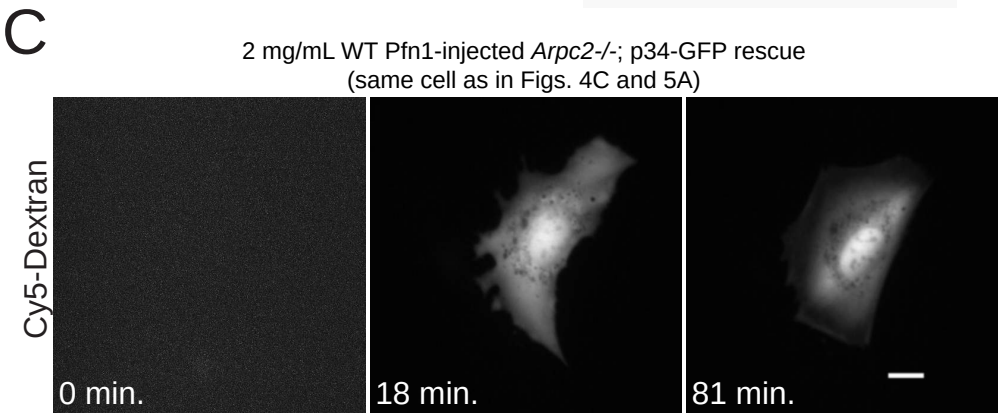

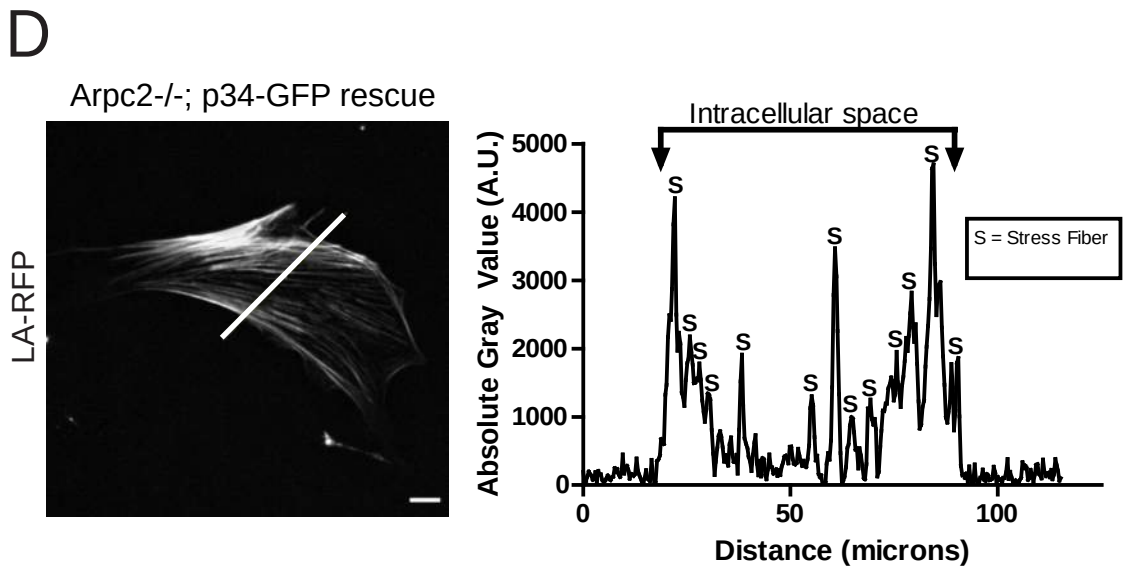

Rotty et al. Supplemental Figure 3

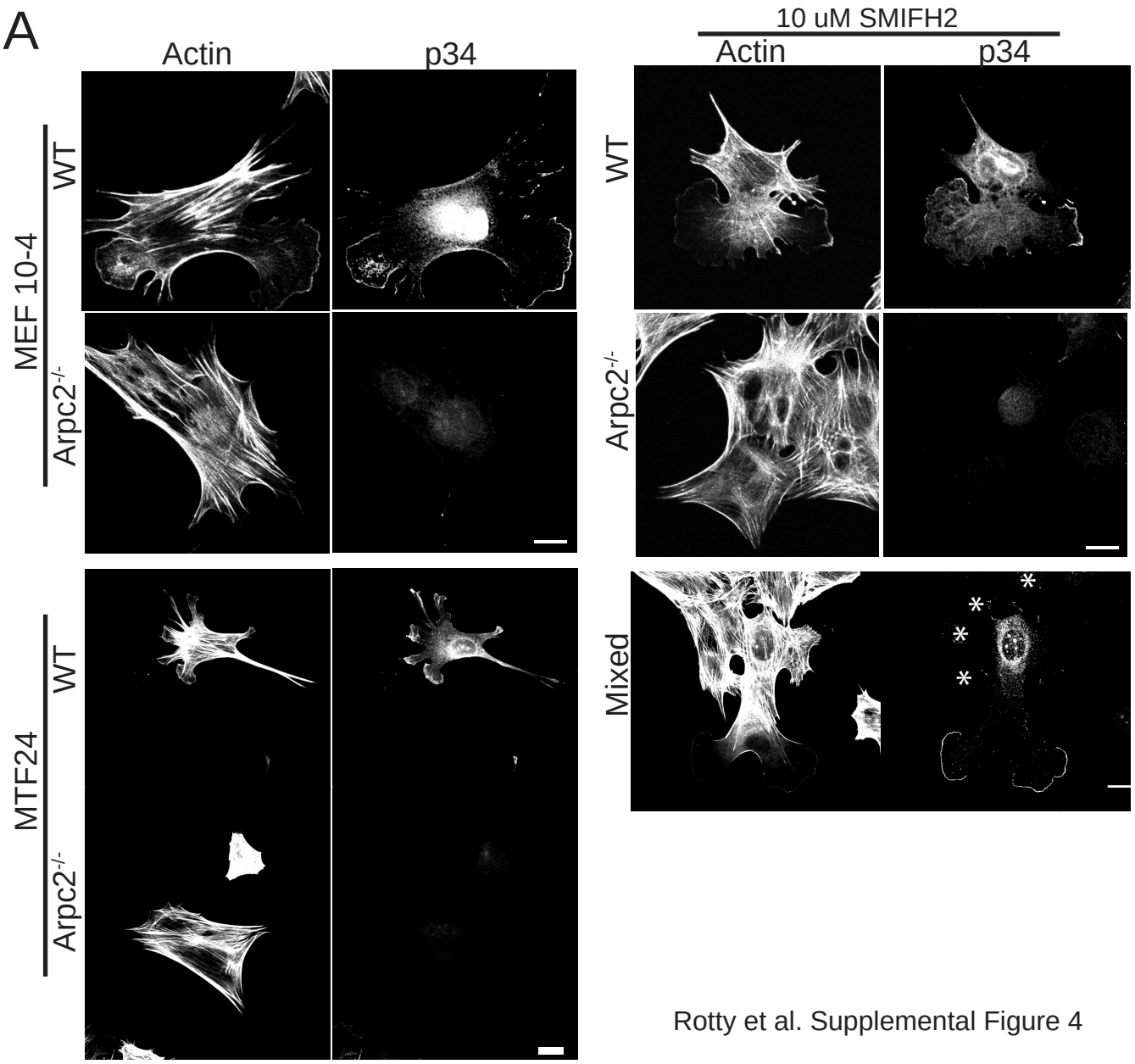

Rotty et al. Supplemental Figure 4

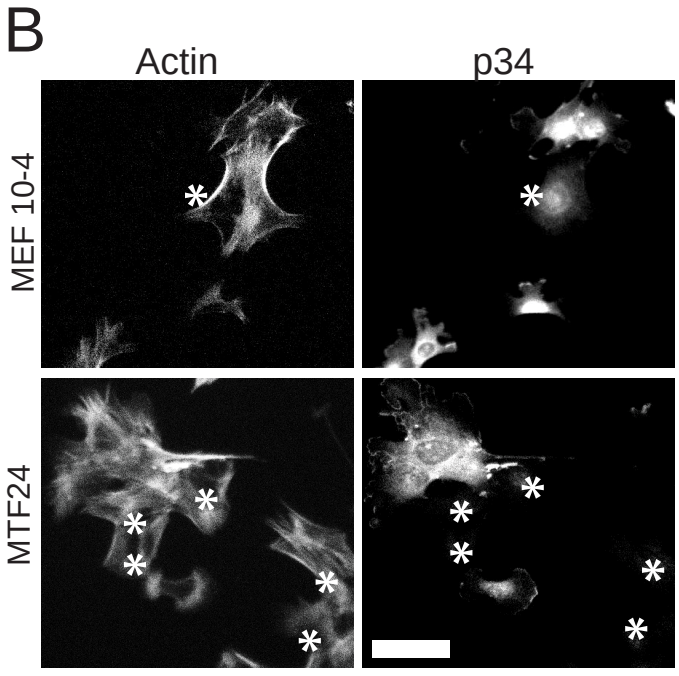

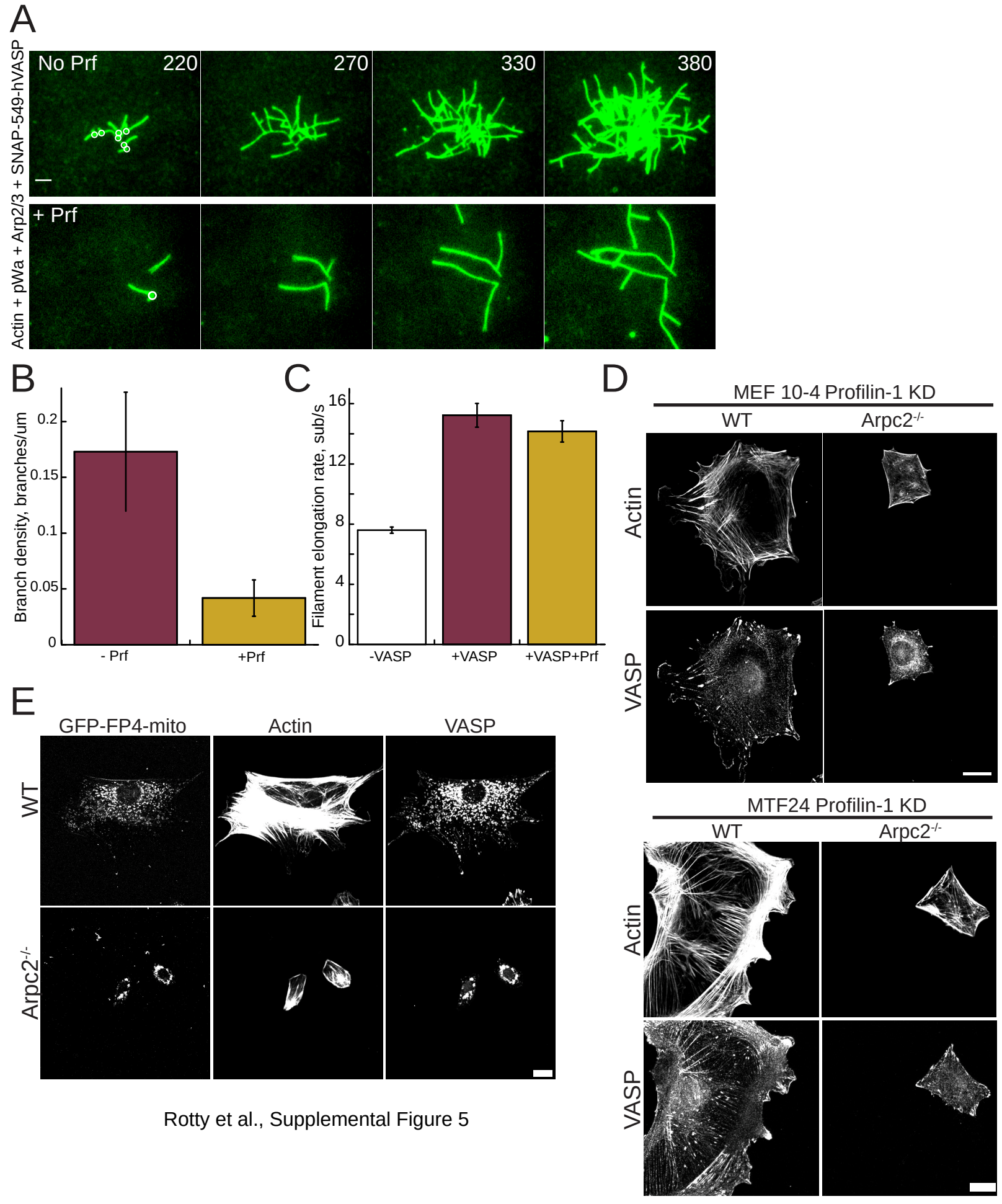

Rotty et al., Supplemental Figure 5

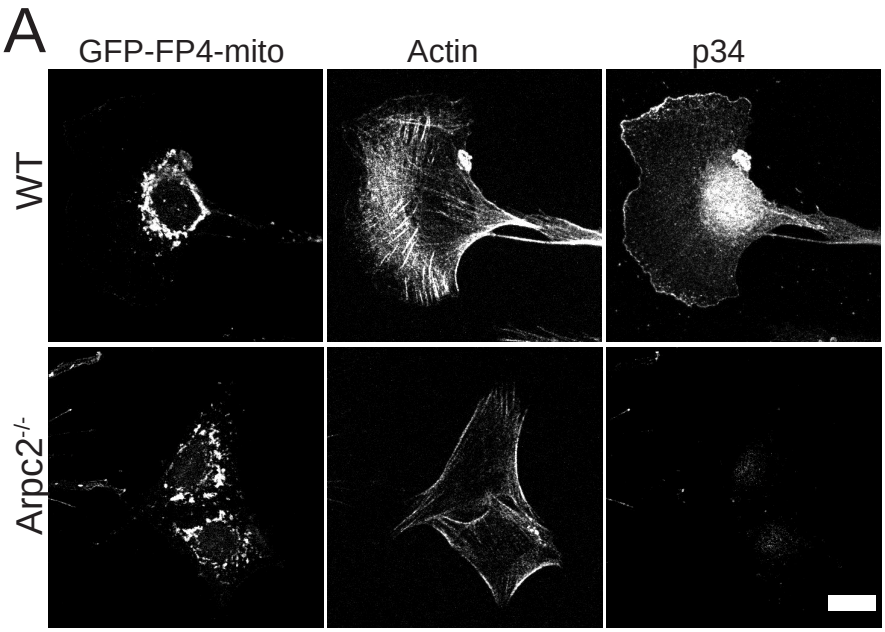

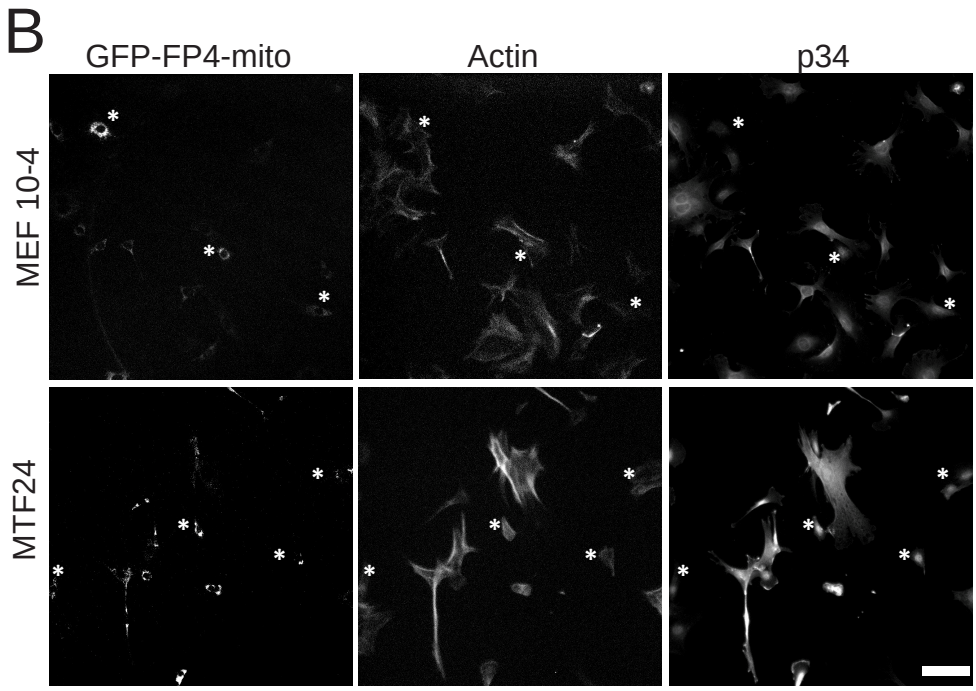

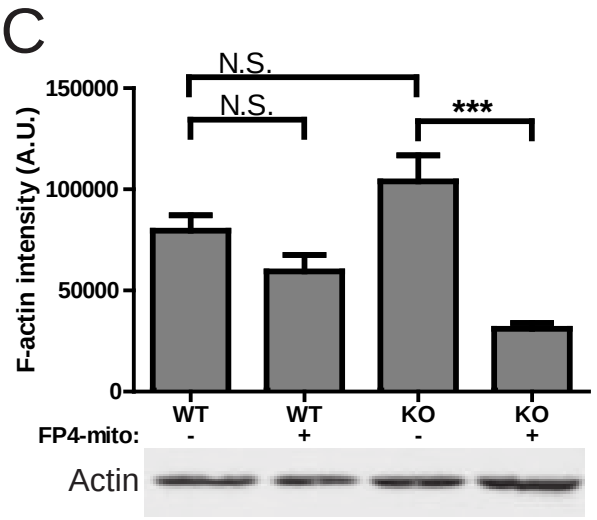

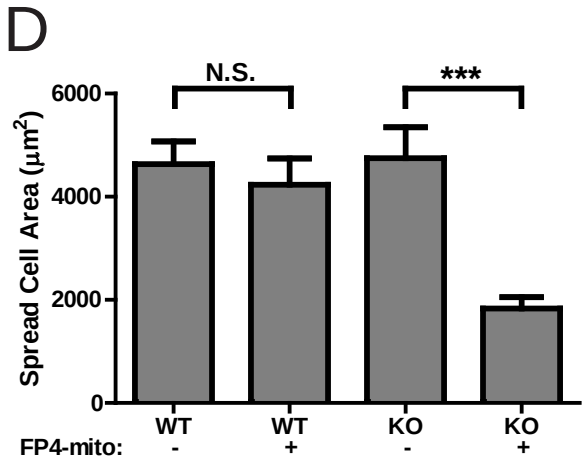

Rotty et al. Supplemental Figure 6

Experimental Procedures:

Mouse strains: C57BL/6 mice with conditional *Arpc2* alleles were ordered from the EUCOMM consortium and mated with mice expressing the FLP recombinase to remove the neomycin selection marker. These mice were then crossed with previously established *Ink4a/Arf-/-* mice (in a mixed genetic background; mice were null for both Ink4a and Arf) (Serrano et al., 1996) and homozygosed to generate $p34^{FL/FL}$; $Ink4a/Arf^{-/-}$ mice in a mixed strain background. All mouse experiments were reviewed and approved by the Institutional Animal Care and Use Committee and were provided with food and water *ad libitum*.

Reagents:

*Antibodies***:** p34 (Millipore), Arp2 (ECM Bio), Arp3 (clone FMS338, Sigma), GAPDH (clone 6C5, Ambion/Life Technologies), vinculin (clone hvin1, Sigma), actin (clone C4, Millipore), profilin-1 (Cell Signaling), VASP (Cell Signaling), Mena (clone A351F7D9, Millipore), secondary antibodies (HRP, cy2, cy5, Rhodamine RedX: Jackson Immunoresearch)

Plasmids: CreER, p34-GFP (in pLL 7.0) (Cai et al., 2008), GFP-FP4-mito (Bear et al., 2000), LA-GFP and LA-RFP (in pLL 5.0) (Vitriol et al., 2007), profilin-1 shRNAs (TRC1 collection, Thermo)

Small molecule reagents: Cytochalasin D (Tocris), Latrunculin B (Sigma), SMIFH2 (Sigma), 4-hydroxy-tamoxifen (Sigma), Alexa 488-, Alexa 568-, or Alexa 647-phalloidin (Life Technologies)

Isolation of fibroblasts: For MTFs, adult mice were sacrificed and tails were harvested and washed with sterile 1X PBS. Syringe needles were used to make a lengthwise incision and the superficial dermis was peeled away. Tail was then diced into small pieces. Culture dishes were coated with gelatin (0.1% gelatin solution at 37°C for 30 minutes). Diced tail pieces were placed into gelatin coated dishes with standard media and culture conditions and allowed to incubate for 3 days, at which point fresh media was added and cells were cultured another 2 days. Tail

tissue was discarded and adherent tail fibroblasts were cultured until confluency in standard media and culture conditions. For MEFs, embryos were collected at E13.5 from mothers set up in timed matings. Uterus and placenta were completely removed and each embryo was chopped coarsely with razorblades, trypsinized in 0.25% trypsin-EDTA for 10 minutes (in 37°C, 5% CO2 incubator), followed by addition of 5 mL DMEM complete (formulation below). Each coarsely disassociated embryo was transferred to separate gentleMACS C Tubes (Miltenyi Biotec) and further disassociated with the gentleMACS Dissociator (Miltenyi Biotec). Bulk cell populations were grown in standard cell culture conditions.

Creation of clonal fibroblast cell lines: Cells were cultured in DMEM (4.5 g/L D-glucose, L-glutamate, 110 sodium pyruvate) supplemented with 10% FBS, 1% Pen/Strep, and 1% Glutamax. Bulk MTF and MEF populations were treated identically to establish clonal lines. CreER was introduced via stable retroviral transduction followed by puromycin selection (2 µg/mL). Single puro-resistant, CreER expressing cells were then sorted into each well of 96 well plates. Growing clones were expanded until confluent in a 10 cm dish and frozen down.

Tamoxifen treatment: Parental MEF 10-4 and MTF24 cells were plated at low density in 6 cm plates in duplicate. After several hours, 2-4 µM of the tamoxifen analogue 4-hydroxy-tamoxifen (4-OHT) was added to one of the two plates, with DMSO to the other, for both lines. Two days later, on day 3, fresh media containing a second identical dose of either 4-OHT or DMSO was added. Two days later, day 5, cells were harvested for lysate, plated for imaging, or expanded for subsequent experiments.

Cell lysis and western blotting: Cells were washed three times with cold 1X PBS and then scraped into ice-cold RIPA buffer: 50 mM Tris pH 8, 150 mM NaCl, 0.5% deoxycholate, 0.1% SDS, 1% NP-40, with 1x concentration of protease and phosphatase inhibitors (PhosStop,

Roche). After transfer, blocking was done for 1 hour in 5% milk (in PBST). Primary antibodies were diluted in 5% milk or 5% BSA, both diluted in PBST, incubated overnight at 4°C. HRP-conjugated secondary antibodies were diluted in 5% milk for 1 hour at room temperature. HRP antibodies were detected via X-ray film or via an imaging machine (Bio Rad), after incubation with developing reagent (Thermo). VASP and Mena relative overexpression was determined using integrated pixel density measurements of band intensity in ImageJ. Values were corrected for loading with GAPDH intensity. Numbers reported are fold change in *Arpc2-/-* compared to matching WT controls.

Immunofluorescence: Cells were plated on acid-washed coverslips coated with 10 µg/mL fibronectin overnight and fixed in cold buffer (solid paraformaldehyde was dissolved to 4% w/v in Krebs-S buffer: 145 mM NaCl, 5 mM KCl, 1.2 mM $CaCl_2$, 1.3 mM $MgCl_2$, 1.2 mM NaH_2PO_4, 10 mM glucose, 20 mM HEPES, 0.4 M sucrose) for 10 minutes at room temperature. Cells were permeabilized in 0.1% Triton X-100 for 5 minutes. Blocking was done in a 1:1 ratio of 10% BSA:10% NGS for 30 minutes at room temperature. Primary antibodies were diluted in 1% BSA and incubated on coverslips for one hour at room temperature. Secondary antibodies were diluted in 1% BSA and incubated on coverslips for 45 minutes at room temperature. Coverslips were mounted in Fluoromount G (Electron Microscopy Sciences).

Confocal microscopy: Confocal Z-stacks of fixed images were obtained on an inverted Fluoview FV1000 scanning confocal microscope (Olympus), using a 0.17 N.A. 40x objective and a Hamamatsu PMT controlled by Fluoview software. Maximum intensity projections were generated from raw .oif files in ImageJ using the ZProject-Maximum Intensity Projection function. Z-stacks were derived from 4-6 individual images taken at one micron intervals. For live imaging, cells were plated on fibronectin-coated (10 µg/mL) glass bottomed Mat-TEK dishes 16 hours before imaging. Cells were maintained at 37°C and 5% CO2 in a closed environmental

chamber attached to the Fluoview FV1000, and imaged with the same objective, camera, and software as fixed images. Images were taken every 15 seconds for 30 frames.

Viral transduction: Retroviral and lentiviral packaging and transduction of mouse fibroblasts were done as described previously (Bear et al., 2000; Cai et al., 2007).

Random motility imaging and analysis: Cells were plated in glass bottomed Mat-TEK dishes on 10 µg/mL fibronectin 6-8 hours before imaging commenced. Cells were imaged every 10 minutes for 12 hours at 10x magnification on an Olympus VivaView FL incubator microscope with a Hamamatsu R2 camera**.** In experiments involving drug treatments, drug was added just prior to imaging and cells remained in the presence of drug for the duration of the experiment. Random velocity of single cells was quantified using the Manual Tracking ImageJ plugin (http://rsbweb.nih.gov/ij/plugins/track/track.html).

F-actin and total actin quantitation: After processing coverslips according to standard lab protocol (above), images were taken on an Olympus IX81 microscope with a 0.30 N.A. 10X objective and an iXon+ front-illuminated EMCCD camera (Andor Technology) and controlled by Metamorph software (Molecular Devices). Images of fluorescent phalloidin were used to determine F-actin content. Briefly, image files were imported into ImageJ and background was subtracted by the program. Cells were carefully outlined by hand and integrated pixel density was measured on a per cell basis to generate average F-actin content per cell. Measurements of the area of outlined cells were generated, and subsequently reported as average spread cell area. As cells were plated for F-actin visualization, a subset of trypsinized cells of the same population (matched at 25,000 cells per condition) were spun down at 1,000xg for 3 minutes at room temperature and whole cell lysates were prepared from pelleted cells. Ten µL of WCL was

used per sample on SDS-PAGE gels. Actin and p34 signal from WCL was simultaneously detected with Li-Cor fluorescent antibodies on an Odyssey detection system (Li-Cor).

Barbed end actin assembly assay: Adapted from Symons and Mitchison (Symons and Mitchison, 1991). Base buffer was diluted from a 5x stock (stock: 100 mM HEPES, 690 mM KCl, 43 mM $MgCl_2$, and 15 mM EGTA). Working buffer was created by adding 2 mM ATP, 2.5 µM unlabeled phalloidin, 0.1 µM labeled phalloidin, and 0.4 µM Alexa 488 actin (Life technologies) to the 1x base buffer. Coverslips were inverted into a droplet of barbed end buffer for 10-60 seconds (control and experimental pairs were treated the same, but optimal time varied among lines), followed by incubation for ten minutes in fixation buffer (solid paraformaldehyde dissolved to 4% w/v in buffer indicated in our immunofluorescence method). Coverslips were then processed with the immunofluorescence protocol previously mentioned in the materials and methods. Experiments using purified profilin-1 (Cytoskeleton) were done identically, except that profilin-1 was included in the complete barbed end buffer at a concentration of 66.5 µM (1 mg/mL).

Cryo-shadowing EM: Nickel grids (200-mesh) covered with a carbon film were treated with a glow discharge at 200 torr for 2 min. FN (50 µg/mL) was used to coat the glowtreated surface for 1 hr at 37 °C. Cells were plated on grids for 2 hr in regular cell culture medium before extraction with extraction buffer (1% Triton X-100 and 2 µM phalloidin in PEM buffer containing 100 mM PIPES, 1 mM EGTA, 1mM MgCl2, pH 6.9) for 4 min at room temperature(Bear et al., 2002). After extraction, cells were rinsed with PEM buffer (pH 6.9) for 1 min and fixed with 1% glutaraldehyde in PBS for 5 min at room temperature. After fixation, grids were briefly rinsed with distilled water and transferred to the chamber of an FEI Vitrobot freezing robot held at 37 °C and 100% humidity(Ozgur et al., 2011). Water remaining on the grid was gently blotted with filter paper before plunging the grid into liquid ethane for rapid freezing. The grids in an

enclosed box under liquid nitrogen were transferred to the stage of a modified Balzers freeze etch machine held at -120 °C. The chamber was evacuated and the sample slowly freeze dried at 1x10-5 to 5x10-7 torr for 4 hr while the temperature was ramped from -120 to -85 °C. The samples were then rotary shadowcast with tungsten prior to breaking the vacuum. The grids were examined in an FEI Tecnai T12 Teat 80 kV. The images were taken with a GATAN Inc Oris 1000 2Kx2K digital camera.

Single Molecule TIRF: Microscope slides (#1.5, Fisher Scientific) were coated with mPEG-Silane (Winkelman et al., 2014). TIRF microscopy images were collected at 5s intervals with an iXon EMCCD camera (Andor Technology) using an Olympus IX-71 microscope equipped with through-the-objective TIRFM illumination. Mg-ATP-actin (1.5 µM, Oregon Green-actin) was combined with the proteins indicated in the text and figure legends in a polymerization mix containing 10 mM Imidazole pH 7.0, 50 mM KCl, 1 mM $MgCl_2$, 1 mM EGTA, 50 mM DTT, 0.2 mM ATP, 50 µM $CaCl_2$, 15 mM glucose, 20 µg/mL catalase, 100 µg/mL glucose oxidase, and 0.5% (wt/vol) methylcellulose 400 centipoise to induce assembly, and transferred to a flow cell. Elongation rates were measured using imageJ, branch densities were calculated by counting the number of branch points and dividing by the total filament length.

Microinjection: Cells were plated overnight in low CO_2 adjustment media (powdered high-glucose DMEM from Sigma was reconstituted according to manufacturer's instructions except that final sodium bicarbonate concentration was 4.4 µM) on Delta-T dishes (Bioptechs) and sealed with parafilm. Cells were removed the next morning and placed into a heated insert for imaging on an Olympus IX81 microscope with a 1.05 N.A. 30X silicon oil objective and an iXon+ front-illuminated EMCCD camera (Andor Technology) and controlled by Metamorph software (Molecular Devices). Several cells were imaged in the GFP, RFP and Cy5 channels prior to microinjection and stage positions were saved. The heated lid was then carefully removed and

saved positions were revisited for microinjection. Microinjection was done using Femtotip needles controlled by the FemtoJet injection controller and InjectMan NI 2 system (all from Eppendorf). Needles were loaded with 2 mg/mL (133 µM) WT or R88E human profilin in profilin buffer (20 mM Tris, pH 7.5; 150 mM KCl; 0.2 mM DTT) plus 0.67 µg/mL Cy5-conjugated dextran (Sigma), or buffer and dextran alone. Using a standard curve of purified His-profilin-1 (Cytoskeleton), we determined the average level of profilin-1 in 2,500 cells to be 5 ng. The corresponding level per cell is 2 pg, or 133.33 amol, profilin-1. We analyzed our cells in suspension and found them to have an average cytoplasmic volume of 4.6 pL. Based on these values, we calculated a cellular profilin-1 concentration of 29 µM, in line with published values in mammalian cells that range from 8.4-50 µM (Finkel et al., 1994; Goldschmidt-Clermont et al., 1991). Though microinjected volume likely differed from cell to cell, the manufacturer's data regarding their femtotip needle reported an injection range of 0.1-0.5 pL. As 0.5 pL is ~10% of cell volume we find it reasonable as an upper bound for injection volume. Given this and the needle concentration of profilin, we could deliver 1 pg (66.67 amol) of profilin. The post-injection concentration of profilin-1 would be 39 µM, an immediate 36% increase in profilin-1 levels. After microinjection, the heated lid was carefully replaced and cells were allowed to re-equilibrate until Z-drift was minimized. Cells at each saved position were imaged every 8 minutes on GFP, RFP and Cy5 channels.

Image analysis: *Actin and Arp2/3 complex edge detection*: The ImageJ Macro Edgeratio (http://www.unc.edu/~cail/code/EdgeRatio.txt) (Cai et al., 2007) was used to measure the distribution of F-actin and p34Arc at the cell edge. The percentage value of the intensity, with the maximal raw value as 1 and the minimal raw value as 0 was plotted with error bars representing SEM. From these data we calculated the average width of the peak intensity in microns. The extreme edge of the cell (0 microns) represents the start of the peak and we

considered anything above cytoplasmic background (the tail of the curve, with an intensity of 0.5) to be part of the peak.

In situ actin assembly quantification: F-actin and Alexa 488-Actin signal was background subtracted, cells were outlined, and fluorescence of both channels was quantified in ImageJ. Barbed end intensity was normalized to total F-actin. Averages of normalized values are reported relative to control WT cells minus profilin.

Arp2/3 complex edge ratio: Confocal stacks of cells imaged on an Olympus FV1000 microscope at 40x were analyzed using MATLAB (MathWorks). Cells were automatically segmented from background via k-means clustering. High Arp2/3 complex signal (designated as intensity greater than 1.2 standard deviations above the mean signal for the whole cell) was analyzed within a 5 pixel band along the cell perimeter. Perimeter area covered by high Arp2/3 complex signal was divided by the total perimeter area of the cell to achieve the final fraction of Arp2/3 complex enriched edge.

Actin stress fiber quantification: Analysis was done similarly to already established approaches (Wei et al., 2011). Briefly, LA-RFP images of *Arpc2-/-* knockout-rescue or *Arpc2-/-* cells were imported into ImageJ and background subtracted. A line was then drawn across the cell perpendicular to the predominant stress fiber orientation. The number of stress fibers intersecting the reference line was quantified from ImageJ line scans or by eye if the intensities were too low to be detected by the software. Three lines were drawn across each injected cell at each time point.

Peripheral lamellipodia length: p34-positive lamellipodia length was analyzed in ImageJ by hand drawing a curved line on top of p34-positive lamellipodial regions. The length of the curved line in microns was measured using the ImageJ software.

Statistical analysis: All means are graphed with standard error of the mean, with the exception of barbed end quantification in which error bars represent 95% confidence intervals. Statistical significance was assessed using unpaired two-tailed t tests, with p-values < 0.05 being considered significant. All statistical tests of raw data were done in GraphPad Prism (GraphPad Software).

Supplemental Figure Legends:

Supplemental Figure 1. Additional characterization of fibroblast cell lines: morphology, F-actin character, response to drug treatment. A) Staining of fixed MEF 10-4 WT and *Arpc2-/-* fibroblasts; scale bar = 20 microns. **B)** Still frames from live cell timecourse of MTF24 WT and *Arpc2-/-* cells stably transfected with the live cell actin probe lifeact (LA)-GFP showing dynamic F-actin behavior in each cell type. Cyan arrowheads depict areas of active protrusion; scale bar = 20 microns. **C**) Representative 10X images of phalloidin (Actin) and p34 used to generate F-actin integrated pixel density measurements from both lines, with WT and KO cells plated in mixed culture for side by side comparison (KO cells denoted by *); scale bar = 100 microns. **D**) Indirect immunofluorescence of fixed MEF 10-4 and MTF24 cells in mixed culture plus 500 nM Latrunculin B (KO cells denoted with *); scale bar = 20 microns. **E)** Staining of fixed MEF 10-4 WT and Arpc2-/- fibroblasts in mixed culture (KO cells marked with *) after addition of 100 nM cytochalasin D (CD) for two hours; scale bar = 20 microns. **F)** Random migration velocity of control (NS) IA32 cells or IA32 cells stably depleted of p34 and Arp2 (2xKD) in the presence or absence of CD. Means are plotted with 95% confidence intervals; N = at least 49 cells per condition, ****p-value < 0.0001. Relates to Figures 1 and 2.

Supplemental Figure 2. Additional characterization of profilin-1 activity in WT and Arp2/3-depleted lines. A) Barbed end assay relating the distribution of labeled barbed ends to total F-actin in control (NS) or Arp2/3 complex depleted (2xKD) IA32 cells in the absence (-) or presence (+) of profilin; scale bar = 10 microns. **B**) Representative 10X images of Pfn1 KD WT and *Arpc2-/-* cells in mixed culture stained for phalloidin (Actin) and p34 (KO cells denoted by *) used to generate F-actin integrated pixel density measurements from both lines; scale bar = 100 microns. **C**) Indirect immunofluorescence of fixed MTF24 WT and Arpc2-/- Profilin-1 KD fibroblasts; scale bar = 20 microns. **D**) Integrated pixel density of phalloidin staining in fixed

MTF24 WT and KO cells ± Pfn1 KD plotted as average F-actin intensity/cell, with SEM. N = 50 cells per condition, ***p-value < 0.0001, **p-value < 0.001. Blots of whole cell lysate matched by cell number directly below. **E)** Spread cell area in sq. microns for MEF 10-4 (black bars) and MTF24 (grey bars) WT and KO cells ± Pfn1 KD, plotted as average area/cell, with SEM. N = 50 cells per condition. ****p-value < 0.0001, ***p-value < 0.0053, **p-value = 0.0124, *p-value = 0.0366. Relates to Figure 3.

Supplemental Figure 3. Image quantification and analysis approaches used for data generation. A) Automated p34 edge detection workflow. Parental image is imported into MATLAB and single cells are detected by the edge analysis program. Steps 2-4 are repeated for each cell detected in the initial analysis step. After step 4, the program calculates the ratio of high p34 edge compared to total cell edge. Scale bar = 20 microns. **B**) Images used for edge detection were also imported into ImageJ and peripheral lamellipodia length in microns was measured for each lamellipodia (outlined in red). Measurements for each example lamellipodia is reported to the right of the image. Scale bar = 20 microns. **C**) Example of Cy5-dextran signal in *Arpc2-/-*; p34-GFP rescue cell from Figs. 4C and 5A, before (0 min) and after microinjection of WT hProfilin-1 at indicated time points. Scale bar = 20 microns. **D**) LA-RFP signal in *Arpc2-/-*; p34-GFP cell. Scale bar = 20 microns. Individual images were background subtracted in ImageJ and straight lines were drawn through the cell perpendicular to the predominant stress fiber orientation (as shown by white line). When signal was detectable above background in ImageJ line traces (example to the right of image), independent peaks of LA-RFP signal were counted (S = stress fiber). Line trace reports Absolute Grey Value vs. distance across the line (in microns), with the section related to intracellular space marked. Relates to Figures 3, 4 and 5.

Supplemental Figure 4. Effect of SMIFH2 on cell morphology, actin organization and F-actin levels. A) Indirect immunofluorescence of fixed MEF 10-4 and MTF24 WT and Arpc2-/-

cells plus or minus SMIFH2; scale bar = 20 microns. **B**) Representative 10X images of WT and Arpc2-/- cells + SMIFH2 in mixed culture stained for phalloidin (Actin) and p34 (KO cells denoted by *) used to generate F-actin integrated pixel density measurements from both lines; scale bar = 100 microns. Relates to Figure 6.

Supplemental Figure 5. Characterization of Ena/VASP interplay with the Arp2/3 complex and confirmation of FP4-mito approach. A) Time-lapse TIRF microscopy of 1.5 µM Oregon green-labeled actin polymerized in the presence of 50 nM Arp2/3 complex, 50 nM pWA, and 20 nM SNAP-549-hVASP without (top) or with (bottom) 5 µM hPRF1. **B**) Effect of Profilin on branch density (branches per micron) in the presence of hVASP and Arp2/3 complex, quantified from time-lapse TIRF experiments in A. Plotted as mean with SEM. **C**) Actin filament elongation rate (subunits/s) in the absence of VASP (-VASP), with VASP alone (+VASP) or with VASP and hProfilin-1 (+VASP/+Prf). Plotted as mean with SEM. **D**) Indirect immunofluorescence of fixed profilin-1 depleted MEF 10-4 and MTF24 WT and *Arpc2-/-* cells for F-actin and VASP localization; scale bar = 20 microns. **E**) Indirect immunofluorescence of fixed MEF 10-4 WT and *Arpc2-/-* fibroblasts, GFP-FP4-mito detected by direct fluorescence rather than antibody. Note VASP localization to mitochondria in FP4-mito (+) cells. Scale bar = 20 microns. Relates to Figure 6.

Supplemental Figure 6. Additional characterization of Ena/VASP involvement in F-actin homeostasis. A) Indirect immunofluorescence of fixed MTF24 WT and *Arpc2-/-* cells transfected with GFP-FP4-mito construct. GFP signal is direct fluorescence, rather than antibody; scale bar = 20 microns. **B**) Representative 10X images of GFP-FP4-mito expressing WT and *Arpc2-/-* cells in mixed culture stained for phalloidin (Actin) and p34 (KO cells denoted by *) used to generate F-actin integrated pixel density measurements from both lines; scale bar = 100 microns. **C**) Integrated pixel density of phalloidin staining in fixed MTF24 WT and KO

cells, or WT/KO cells stably expressing FP4-mito-GFP (FP4-mito +), plotted as average F-actin intensity/cell, with SEM. N = 50 cells per condition; ***p-value < 0.0001. Western blots of whole cell lysate matched by cell number directly below. **D**) Spread cell area in sq. microns of MTF24 WT, WT FP4-mito, KO and KO FP4-mito cells plotted as average area/cell with SEM. N = at least 50 cells per condition; ***p-value < 0.0001. Relates to Figure 6.

Supplementary Movie Legends:

Movie S1. Time lapse imaging of LA-GFP labeled actin in MEF 10-4 WT or *Arpc2-/-* cells. Time lapse imaging of Lifeact (LA)-GFP labeled actin in MEF 10-4 WT (left) or *Arpc2-/-* (right) cells corresponding to Figure 2D still frames. Images were taken every 15 seconds for 435 seconds. Imaging was done at 37°C with 40X magnification in 5% CO_2. Scale bar = 20 microns. Relates to Figure 2.

Movie S2. Time lapse imaging of LA-GFP labeled actin in MTF24 WT or *Arpc2-/-* cells. Time lapse imaging of LA-GFP labeled actin in MTF24 WT (left) or *Arpc2-/-* (right) cells corresponding to Figure S1C still frames. Images were taken every 15 seconds for 435 seconds. Imaging was done at 37°C with 40X magnification in 5% CO_2. Scale bar = 20 microns. Relates to Figure S1.

Supplementary Literature Cited

Bear, J., Loureiro, J., Libova, I., Fassler, R., Wehland, J., and Gertler, F. (2000). Negative regulation of fibroblast motility by Ena/VASP proteins. Cell *101*, 717-728.

Bear, J.E., Svitkina, T.M., Krause, M., Schafer, D.A., Loureiro, J.J., Strasser, G.A., Maly, I.V., Chaga, O.Y., Cooper, J.A., Borisy, G.G*., et al.* (2002). Antagonism between Ena/VASP Proteins and Actin Filament Capping Regulates Fibroblast Motility. Cell *109*, 509-521.

Cai, L., Makhov, A.M., Schafer, D.A., and Bear, J.E. (2008). Coronin 1B antagonizes cortactin and remodels Arp2/3-containing actin branches in lamellipodia. Cell *134*, 828-842.

Cai, L., Marshall, T.W., Uetrecht, A.C., Schafer, D.A., and Bear, J.E. (2007). Coronin 1B coordinates Arp2/3 complex and cofilin activities at the leading edge. Cell *128*, 915-929.

Finkel, T., Theriot, J.A., Dise, K.R., Tomaselli, G.F., and Goldschmidt-Clermont, P.J. (1994). Dynamic actin structures stabilized by profilin. Proc Natl Acad Sci U S A *91*, 1510-1514.

Goldschmidt-Clermont, P.J., Machesky, L.M., Doberstein, S.K., and Pollard, T.D. (1991). Mechanism of the interaction of human platelet profilin with actin. J Cell Biol *113*, 1081-1089.

Ozgur, S., Damania, B., and Griffith, J. (2011). The Kaposi's sarcoma-associated herpesvirus ORF6 DNA binding protein forms long DNA-free helical protein filaments. J Struct Biol *174*, 37-43.

Serrano, M., Lee, H., Chin, L., Cordon-Cardo, C., Beach, D., and DePinho, R.A. (1996). Role of the INK4a locus in tumor suppression and cell mortality. Cell *85*, 27-37.

Symons, M.H., and Mitchison, T.J. (1991). Control of actin polymerization in live and permeabilized fibroblasts. J Cell Biol *114*, 503-513.

Vitriol, E.A., Uetrecht, A.C., Shen, F., Jacobson, K., and Bear, J.E. (2007). Enhanced EGFP-chromophore-assisted laser inactivation using deficient cells rescued with functional EGFP-fusion proteins. Proc Natl Acad Sci U S A *104*, 6702-6707.

Wei, S., Gao, X., Du, J., Su, J., and Xu, Z. (2011). Angiogenin enhances cell migration by regulating stress fiber assembly and focal adhesion dynamics. PLoS One *6*, e28797.

Winkelman, J.D., Bilancia, C.G., Peifer, M., and Kovar, D.R. (2014). Ena/VASP Enabled is a highly processive actin polymerase tailored to self-assemble parallel-bundled F-actin networks with Fascin. Proc Natl Acad Sci U S A.